



# Nonstoichiometry of ZnGeP<sub>2</sub> crystals probed by static tensimetric method

I.G. Vasilyeva<sup>a,\*</sup>, R.E. Nikolaev<sup>a</sup>, G.A. Verozubova<sup>b</sup>

<sup>a</sup> Nikolaev Institute of Inorganic Chemistry, Russian Academy of Sciences, Siberian Branch, 3, Acad. Lavrentyev Pr. Novosibirsk 630090, Russia

<sup>b</sup> Institute of Monitoring of Climatic and Ecological Systems, Russian Academy of Sciences, Siberian Branch, 10/3, Akademicheskyy Pr., Tomsk 634055, Russia

## ARTICLE INFO

### Article history:

Received 17 May 2010

Received in revised form

12 July 2010

Accepted 18 July 2010

Available online 3 August 2010

### Keywords:

ZnGeP<sub>2</sub> nonstoichiometry

XRD

Density

Static tensimetric method

## ABSTRACTS

The nonstoichiometry of ZnGeP<sub>2</sub> has been determined based on the  $p$ - $T$  dependences measured above ZnP<sub>2</sub>-Ge samples in the temperature range of 980–1225 K by a high-sensitive and precise tensimetric static method with a quartz Bourdon gauge. Scanning of the compositional range 49–51 mol% ZnP<sub>2</sub> in the closed system and construction of the  $p$ - $T$  dependences were possible due to incongruent evaporation of ZnGeP<sub>2</sub> and formation of volatile species Zn(g), P<sub>4</sub>(g) and P<sub>2</sub>(g). The maximum homogeneity range of the solid ZnGeP<sub>2</sub> was determined between 50.03 and 49.61 mol% ZnP<sub>2</sub> at a temperature of 1128 K, based on the inflection points on the  $p$ - $T$  dependences, corresponding to transitions of the three-phase (solid–solid–vapor) equilibrium to a two-phase (solid–vapor) one and vice versa. The nonstoichiometry as the overall concentration of defects is considered to gain a better insight into the defect chemistry of ZnGeP<sub>2</sub>.

© 2010 Elsevier Inc. All rights reserved.

## 1. Introduction

ZnGeP<sub>2</sub> (ZGP) is known as one of the most promising infrared nonlinear optical materials [1,2]. However, a lack of the high-quality single crystals limits a wide application of ZGP crystals. A main factor of the limitation is deviation from stoichiometry of ZGP that appears because of the incongruent evaporation. The Zn and P components are readily evaporated from ZGP, producing a vapor pressure within 3.5–4.2 bar at the melting temperature according to [3,4]. It is expected that the homogeneity range of the solid ZGP is mostly pronounced along the quasi-binary ZnP<sub>2</sub>-Ge section of the ternary Zn-Ge-P diagram. Several studies of the ZGP nonstoichiometry have been carried out using differential thermal and X-ray analyses [5–8]. ZGP can dissolve 1 or 10% of Ge and ~1 mol% ZnP<sub>2</sub>, and ZGP is a phase of variable composition [5–8]. On the other hand, some properties show evidence that ZGP is a typical linear phase [7]. From photoluminescence, photoconductivity, and optical absorption it was determined that concentration of phosphorus and zinc vacancies may be of the order  $\sim 10^{19} \text{ cm}^{-3}$  [6,9], but there is little reason for assigning the concentration to a limiting value of solid solubility of ZnP<sub>2</sub> and Ge in ZGP. These conflicting results demonstrate that the classic techniques mentioned are not sensitive enough to determine the real nonstoichiometry of the incongruently evaporating ZGP.

A most promising static tensimetric method, determining precisely a narrow homogeneity range of ZGP, was used with a quartz Bourdon gauge, measuring the vapor pressure in equilibrium with the crystals [10]. Owing to incongruent evaporation in

the closed system the starting crystals vary gradually in composition with temperature, and on the  $p$ - $T$  dependences transitions from three-phase (solid–solid–vapor) to the two-phase (solid–vapor) equilibrium occur as the inflection points. At these points (complete evaporation of one of the two solid phases) the vapor phase is in equilibrium with the crystals of the boundary composition. We expected that this method would be able to determine the homogeneity range of the solid ZGP as 0.02–0.03 at%. The results of the investigation have a great significance to gain a better insight into the defect chemistry of ZGP.

## 2. Experimental procedures

ZnP<sub>2</sub>-Ge alloys with nominal composition 49.0, 49.5, 50.5, and 51.0 mol% ZnP<sub>2</sub> were prepared via fusion. The starting materials were the nominally stoichiometric ZGP (1.00000 g), prepared previously by the manner given in [11] with additions of the high-purity Ge (0.01453, 0.00727 g) or ZnP<sub>2</sub> (0.01274, 0.02547 g). The mixtures were placed in a cleaned by Aqua Regia quartz ampoule, which then were evacuated and sealed. The synthesis of the alloys was performed in a rotary furnace at 1333 K for 8 h, and then the stepped lowering of furnace temperature was made with different rates down to 773 K. At this temperature the furnace was switched off. To attain equilibrium, the thermal annealing was carried without opening of the ampoules at 873 K for 400 h with a subsequent slow cooling to room temperature. A 50.0 mol% ZnP<sub>2</sub> sample weighing 5.6 g was cut from a nominally stoichiometric single ingot, thermally annealed [12].

The density of produced bulk samples (before powdering) was measured by hydrostatic weighing in ethanol [13] within an estimated error of  $\times 0.0005 \text{ g/cm}^3$ . Analysis of the stoichiometric

\* Corresponding author. Fax: +7 383 330 9489.

E-mail address: kamarz@niic.nsc.ru (I.G. Vasilyeva).

sample with an EDX-equipped JEOL JSM-6700 F SEM, showed its spatial homogeneity. Other samples were crushed, grinded and mass-averaged. Doing this, we ensured identity in composition of small portions and the bulk sample.

The elemental composition of the samples was examined by inductively coupled plasma atomic emission spectrometry (ICP AES) after dissolution of 0.015 g in a single-chamber autoclave at a temperature of 220 °C using an acid mixture with ratio  $\text{HNO}_3:\text{HCl}:\text{H}_2\text{O}=15:5:10$ . This solvent was effective to oxidize fully the volatile species  $\text{PH}_3$  and to keep the  $\text{Ge}^{4+}$  ions in solutions without their precipitation as  $\text{GeO}_2 \cdot \text{H}_2\text{O}$ . Details of the analytical procedure developed by us will be published in another journal. X-ray powder diffraction data of the sample fragments were collected with a diffractometer DRON-UM1 using  $\text{CuK}\alpha$  radiation, by step width of  $0.04^\circ$  and quartz as an external standard. Lattice constants were refined by a full profile analysis of all reflections, and of individual ones (260) at  $2\theta=126.29^\circ$  and (3110) at  $2\theta=115.60^\circ$  using Cell Program, Version 03.12.2003.

The total vapor pressure above the samples was measured by means of a quartz Bourdon gauge with a plate-shaped membrane as a null-point instrument. The limits of this set up are 1170 K in temperature and 2 bar in pressure. The gauge chamber was placed into a two-zone furnace with an isothermal profile ( $\pm 0.5$  K). The vapor pressure above the sample in the chamber was balanced by equal pressure of argon that was measured by U-shaped manometer with accuracy of  $1.3 \times 10^{-4}$  bar and readings were made through a KM-8 type cathetometer. Step-by-step heating and cooling procedures were used. The accuracy of the temperature measurements was about 2 K, of the vapor pressure  $1.3\text{--}2.7 \times 10^{-3}$  bar and of the mass  $\sim 10^{-5}$  g, allowing a determination of the homogeneity range of ZGP about 0.03 mol%  $\text{ZnP}_2$ .

### 3. Results and discussion

#### 3.1. Characterization of samples

The result of the chemical analysis of the samples are 50.6; 50.3, 50.0, 49.6 and 48.9 mol%  $\text{ZnP}_2$  with an error of  $\times 0.2\%$ . The real compositions as more realistic differed from the nominal

ones in the case of the nonstoichiometric samples, losing weekly bonded surface layers in a small amount before characterization. The following symbols of samples are used: Zn-2 (50.6%), Zn-1(50.3%), Zn-0 (50.0%), Ge-1 (49.6%), and Ge-2 (48.9%).

The X-ray powder pattern is shown in Fig. 1 for Zn-2 sample. Here the only impurity peak at  $2\theta=26\text{--}27^\circ$  was indexed as the peak of maximum intensity of the tetragonal  $\text{ZnP}_2$  phase (ICSD card 018137). For all other samples the patterns have no impurity peaks and showed structure belonging to the space group  $I\bar{4} 2d$  (ICSD card 023706). It seems that XRD method is not sensitive enough to detect  $\leq 0.5$  mol%  $\text{ZnP}_2$  and 1.0 at% Ge. The  $a$  and  $c$  unit cell parameters as a function of the composition are shown in Fig. 2. No change was found of the  $a$  parameter for ZGP with increasing of  $\text{ZnP}_2$  content, while the parameter  $c$  increased. Insolubility of  $\text{ZnP}_2$  in solid  $\text{ZnGeP}_2$  is a possible explanation of the constant value of the  $a$  parameter, while the change of the  $c$  parameter is more often related to a layer distortion [6]. The  $a$  and  $c$  parameters vary visibly as compared with Zn-0 only for Ge-1 and stay without variation for Ge-2. Such behavior of the lattice parameters with composition is an indication of solubility of Ge in the solid ZGP. But the conclusion is not enough reliable because of a very small change of the lattice parameters and the absence of the Ge peaks on the X-ray patterns of samples Ge-1 and Ge-2.

A further understanding of phase purity of the samples was got from precise measurement of experimental density, comparing with density calculations from the structural data. Calculation of density was done in the model of the homogeneous solid solutions  $\text{ZnGe}_{1+x}\text{P}_2$ ,  $\text{Zn}_{1+x}\text{GeP}_{2+2x}$ , and in the model of two-phase mixtures,  $\text{ZnGeP}_2+\text{Ge}$  and  $\text{ZnGeP}_2+\text{ZnP}_2$ . Fig. 3 shows that the experimental density agrees well with density of the two-phase mixtures within the measurement accuracy. The experimental density was further used to calculate the quantity of each phase in the mixtures  $P_{\text{mix}} = P_{\text{ZnGeP}_2} + P_{\text{ZnP}_2}$  and  $P_{\text{mix}} = P_{\text{ZnGeP}_2} + P_{\text{Ge}}$  using equation from [13]:

$$x = P_{\text{mix}} \frac{D_1(D_2 - D_{\text{mix}})}{D_{\text{mix}}(D_2 - D_1)}, \quad (1)$$

where  $P_{\text{mix}}$  is a weight of the sample in g,  $D_{\text{mix}}$  is the experimental density,  $D_2$  is density of  $\text{ZnGeP}_2$  equal to  $4.153 \text{ g/cm}^3$ ,  $D_1 = 3.50 \text{ g/cm}^3$  is density of  $\text{ZnP}_2$ , as well as  $D_1 = 5.32 \text{ g/cm}^3$  is density of Ge.

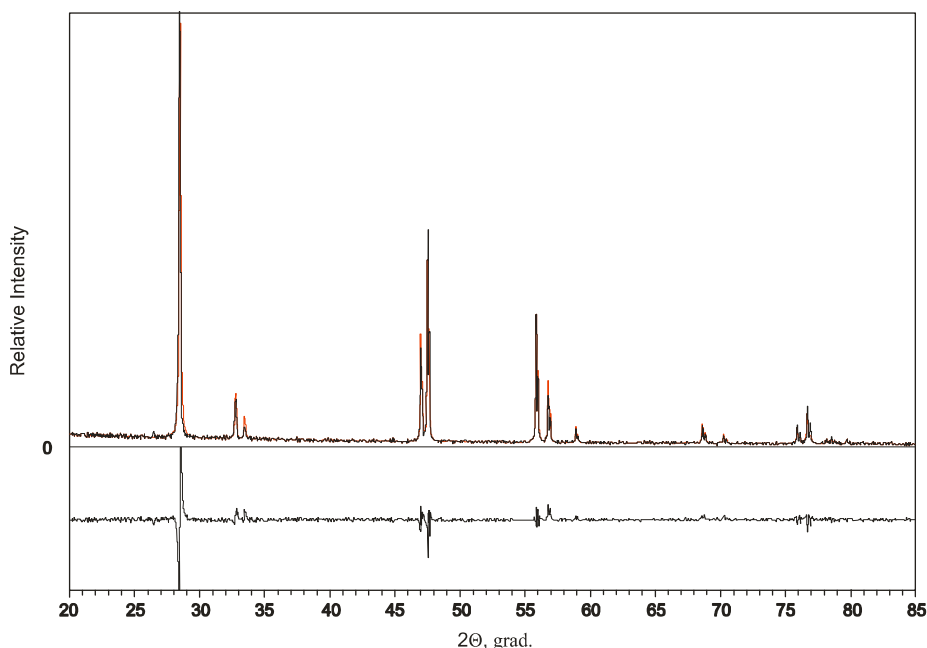


Fig. 1. X-Ray diffraction patterns for the sample Zn-1 with 50.6 mol%  $\text{ZnP}_2$ .

The results are given in Table 1, and are in good agreement between compositions calculated by this way (last column) and those determined chemically (first column), that provides a reliability of these experimental values.

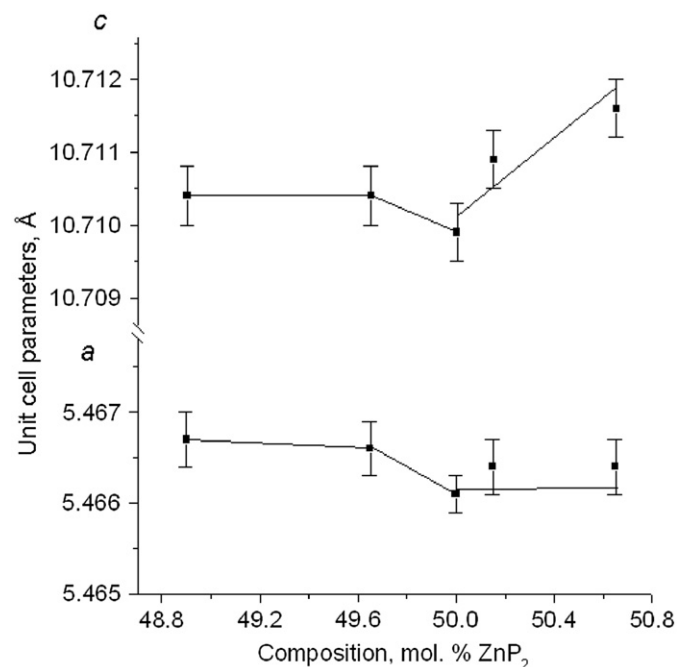


Fig. 2. The change of unit cell parameters with composition of the samples deviated from the ZGP stoichiometry.

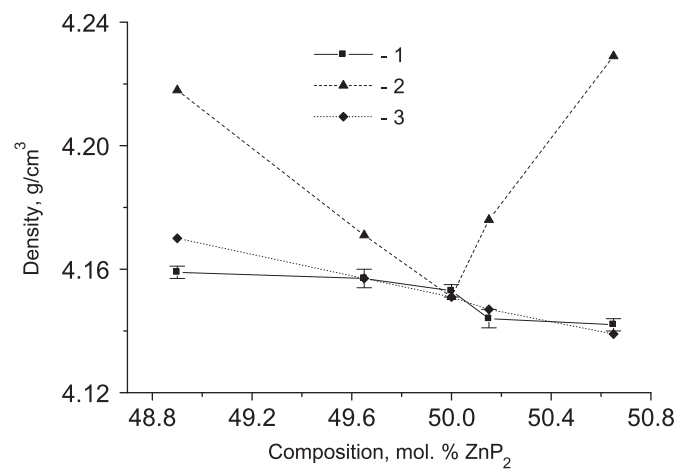


Fig. 3. Experimental (1) and calculated density of the samples in the model of solid solutions (2) and in the model of the phase mixture (3).

Table 1  
Main characteristics of the prepared samples.

| Sample/nominal composition, mol% ZnP <sub>2</sub> | Chemical composition (ICP AES), mol% ZnP <sub>2</sub> ± 0.2 | Experimental density, g/cm <sup>3</sup> ± 0.002 | Unit cell parameters (Å) |             | Composition from density, mol% ZnP <sub>2</sub> ± 0.2 |
|---|---|---|--------------------------|-------------|---|
|   |   |   | a, ± 0.0003              | c, ± 0.0004 |   |
| Ge-2/49.0   | 48.9  | 4.159   | 5.4667                   | 10.7104     | 48.8  |
| Ge-1/49.5   | 49.6  | 4.157   | 5.4666                   | 10.7104     | 49.5  |
| Zn-0/50.0   | 50.0  | 4.153   | 5.4661                   | 10.7091     | 50.0  |
| Zn-1/50.5   | 50.3  | 4.144   | 5.4664                   | 10.7109     | 50.5  |
| Zn-2/51.0   | 50.6  | 4.142   | 5.4664                   | 10.7116     | 50.6  |

### 3.2. Tensimetric measurements

It was previously shown [3,5] that the vapor above all samples in the ZnP<sub>2</sub>–Ge system is mainly consisted of Zn and P species. Therefore, the initial composition of the solid samples evaporating in the closed system will be shifted to the Ge side. Taking different weights (*m*) of a sample and a different chamber volume (*V*), it was possible to pass from the three-phase equilibrium S<sub>ZnP<sub>2</sub></sub>S<sub>ZGP</sub>G to the two-phase one S<sub>ZGP</sub>G and then again to three-phase equilibrium S<sub>ZGP</sub>S<sub>Ge</sub>G by heating the sample. Such transitions appear as inflection points on the *p*–*T* curves. Calculating the vapor weight and the number of moles N<sub>ZnP<sub>2</sub></sub><sup>v</sup> in the vapor at these points with given *p* and *T* coordinates from formula (ideal gas law):

$$m_v = \frac{pVM_v}{RT}, \quad (2)$$

it is possible to find the boundary compositions of the homogeneity range of ZGP from both ZnP<sub>2</sub> and Ge sides knowing weight and composition of the starting sample. In this case the necessity arises to determine the partial pressures of all gaseous species and the vapor composition M<sub>v</sub> in these points, since all other values are experimentally measured.

Results of six (#1–6) tensimetric experiments, measuring the vapor pressure above the samples with different composition and concentration are given in Fig. 4, where three A, B and C curves show several inflection points, corresponding to change of the phase state in the system. The total vapor pressure above the Zn-1 and Zn-2 samples (#1 and #2) falls first on the straight line A, which does not differ from the saturated vapor pressure of the pure ZnP<sub>2</sub> according to [14,15]. It means that both the samples Zn-2 and Zn-1 are two-phase mixtures, and the lower part of the line A reflects the three-phase equilibrium S<sub>ZGP</sub>S<sub>ZnP<sub>2</sub></sub>G (solid ZnP<sub>2</sub>, ZnP<sub>2</sub>-saturated solid ZGP and gas). An analytical equation of the three-phase equilibrium with standard dispersion is given in Table 2 together with the lg *p*–1/*T* dependence of the pure ZnP<sub>2</sub> (first and second rows).

In points 1' and 2' the full decomposition of the solid ZnP<sub>2</sub> takes place and the two-phase equilibrium S<sub>ZnP<sub>2</sub></sub>G occurs that is kept until the complete evaporation of ZnP<sub>2</sub> in the points 1'' and 2'' with the formation of a homogeneous gaseous phase. To determine the boundary compositions of the ZGP homogeneity range from the ZnP<sub>2</sub> side in the inflection points 1'' and 2'' the vapor composition and the ZnP<sub>2</sub> quantities were calculated. Our attempts to determine thermodynamically the vapor composition, employing the Gibbs free energy minimization technique via the program "Equilibrium", analog of EUROTERMA [16] were unsuccessful, because of large scattering in values of the starting thermodynamic data for solid ZnP<sub>2</sub> and Zn<sub>3</sub>P<sub>2</sub> according to [4,5]. Reliable data of the following evaporation reactions:





were obtained using the following system of the equations:

$$p = p_{\text{Zn}} + p_{\text{P}_4} + p_{\text{P}_2} \text{ as total pressure at the inflection points} \quad (7)$$

$$K_{\text{equilib.}} \text{ of the reaction (6) for given temperatures taken from [15]} \quad (8)$$

$$p_{\text{Zn}} = 2P_{\text{P}_4} + P_{\text{P}_2} \text{ due to molar Zn/P ratio equal to } \sim 0.5[3] \quad (9)$$

The composition error was calculated applying the error accumulation law and assuming “exact” values of starting compositions and equilibrium constant  $K_{\text{equilib.}}$ . The errors of measurement of  $T$ ,  $p$ ,  $V$  and the sample mass were known from each the tensimetric experiment. The results of the calculations for experiments #1 and #2 as well as #3 and #4 (see below) are given in Table 3. Note that the real value of the vapor pressure is determined with some addition ( $p + \Delta p$ ) because of uncontrolled volatile by-products and the membrane deformation in the temperature interval. This uncertainty reduced accuracy of the calculated values of the boundary composition (Table 3).

From experiments #1 and #2 it is clear that ZGP dissolves small amounts of  $\text{ZnP}_2$ :  $\sim 0.02$ – $0.03\%$  taking into account the much less precision of the first value. This conclusion is supported by the fact that the vapor pressure above the stoichiometric sample at any temperature on the curve  $B$  lying into the two-phase solid–vapor region is always less than the pressure of the three-phase line  $A$  with the 50.5% sample.

The vapor pressure above the samples Ge-1 (49.6%) and Ge-2 (48.9%) with a density  $m/V$ , equal to 0.00778 and 0.00771 g/ml,

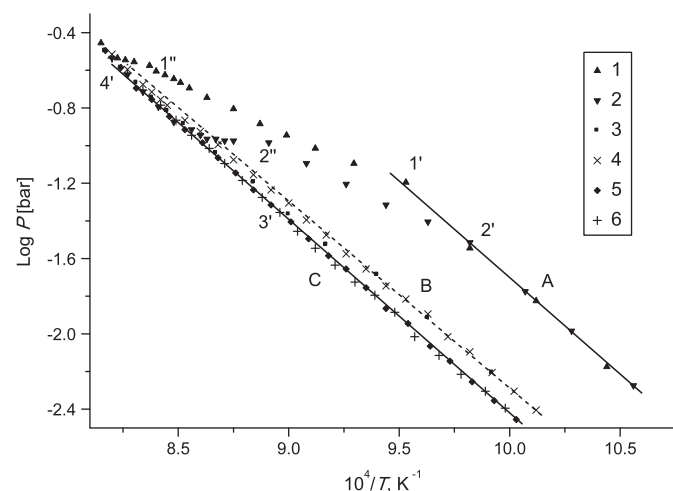


**Fig. 4.** Dependences of the vapor pressure from temperature for all tensimetric experiments: 1—50.6 mol%  $\text{ZnP}_2$ ,  $m/V=0.00936$  g/ml; 2—50.5 mol%  $\text{ZnP}_2$ ,  $m/V=0.00774$  g/ml; 3—50.0 mol%  $\text{ZnP}_2$ ,  $m/V=0.00187$  g/ml; 4—50.0 mol%  $\text{ZnP}_2$ ,  $m/V=0.03279$  g/ml; 5—49.7 mol%  $\text{ZnP}_2$ ,  $m/V=0.00778$  g/ml; and 6—48.9 mol%  $\text{ZnP}_2$ ,  $m/V=0.00701$  g/ml.

**Table 2**

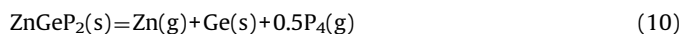
Temperature dependences of total vapor pressure along the monovariant lines.

| Equilibrium  | Equation in bar and temperature interval                  | Reference                 |
|--|---|---------------------------|
| $S_{\text{Zn}}S_{\text{ZnP}_2}G$ (line A)                          | $\lg p$ (Torr) = $-(10750 \pm 230)/T + (11.92 \pm 0.22)$  | 958–1018 K<br>This study  |
| $S_{\text{ZnP}_2}G$  | $\lg p$ (Torr) = $-(9820 \pm 270)/T + (11.01 \pm 0.28)$   | 890–1160 K<br>[12]        |
| $S_{\text{ZnGeP}_2}S_{\text{s,s}}G$ (line B)                       | $\lg p$ (Torr) = $-(10080 \pm 286)/T + (10.68 \pm 0.28)$  | 988–1049 K<br>This study  |
| $S_{\text{ZnGeP}_2}S_{\text{s,s}}G$                                | $\lg p$ (Torr) = $-(10543 \pm 276)/T + (11.09 \pm 0.236)$ | 1053–1243 K<br>[3]        |
| $S_{\text{ZnGeP}_2}S_{\text{Ge}}G$ (line C) of experiments 5 and 6 | $\lg p$ (Torr) = $-(10387 \pm 53)/T + (7.94 \pm 0.05)$    | 1028–1203 K<br>This study |
| Line C of experiments 3–6  | $\lg p$ (Torr) = $-(10325 \pm 155)/T + 7.91 \pm 0.13$     | 1153–1203 K<br>This study |

respectively (experiments #5 and #6), is moving along a straight line in a wide temperature range and describing by analytical equation given in Table 2 (fifth row). The monovariant character of the line corresponds to the three-phase equilibrium  $S_{\text{ZnGeP}_2}S_{\text{Ge}}G$ , meaning that the ZGP homogeneity range from the Ge side may be estimated as  $\leq 0.4$  mol%  $\text{ZnP}_2$ .

More precisely the boundary compositions were determined based on the  $p$ – $T$  dependences, measured above the stoichiometric sample Zn-0 with different ratio  $m/V$  (experiments #3 and #4). It can be seen that curve  $B$  lies within the two-phase range and the pressures at each temperature on this line are less than pressure on the three-phase equilibrium curve  $A$  but larger than that on the three-phase equilibrium curve  $C$ . But the pressure of the samples with  $m/V$  equal to 0.00187 and 0.03279 g/ml falls on this line only at the beginning, until initial composition of ZGP, as a phase of a variable composition, stays fixed. An analytical equation of the homogeneous part of the line  $B$  corresponding to the three-phase equilibrium  $S_{\text{ZnGeP}_2}S_{\text{s,s}}G$  is given in Table 2 (third row) that is close to the equation (fourth row) given in [3]. Now the exact value of the equilibrium pressure of  $\text{ZnP}_2$  under the strict stoichiometric solid ZGP at any temperature is coming to light. We emphasize that the extrapolation of these lines to the melting point of the stoichiometric ZGP having no solid–solid phase transition [6] gives the total pressures equal to 1.29 and 1.47 bar, respectively. Therefore, the pressure of 4.21 bar given in [3] as the decomposition pressure of ZGP at melting point stays questionable without explanation how it was measured. We think that preference should be given to the first values as more realistic ones.

The  $\lg p - 1/T$  dependences above Zn-0 in experiments #3 and #4 with small and large the  $m/V$  values begin to deviate from the straight line  $B$  at 1000 and 1060 K, respectively, to move further along individual polythermic curves until intersection with the three-phase line  $C$ . With a further temperature increase the vapor pressures vary along the line of the three-phase  $S_{\text{ZnGeP}_2}GeG$  equilibrium measured in experiments #5 and #6. It means that the lower boundary of ZGP homogeneity from the Ge side is restricted by the 49.6% composition determined chemically (sample Ge-1). The boundary compositions from the Ge side were also calculated at the intersection points, following the thermal dissociation reactions of ZGP [3]:



The vapor composition at these points was calculated using Eqs. (7)–(9), and the solid solubility of Ge in ZGP was found to be 49.59(9) at 1064 K and 49.69(9) mol% at 1225 K, Table 3 (the third and fourth rows). These values are within the error of the tensimetric experiments agreed with the composition determined chemically as 49.6% for the sample Ge-1. Convergence of the results obtained by two independent methods (chemical and tensimetric) confirms the correctness of the values. Note that similar calculations can be done for any fixed composition within

**Table 3**  
The boundary compositions of ZGP homogeneity range from ZnP<sub>2</sub> and Ge sides.

| Tensimetric experiment/the sample Ratio $m/V$ , g/ml | Composition, mol% ZnP <sub>2</sub> | The vapor composition (bar) |                |                | Boundary composition, mol% ZnP <sub>2</sub> |
|--|------------------------------------|-----------------------------|----------------|----------------|---|
|  |                                    | Zn                          | P <sub>4</sub> | P <sub>2</sub> |   |
| #1/Zn-2<br>$9.36 \times 10^{-3}$                     | 50.6                               | 0.152                       | 0.065          | 0.022          | 49.77 (25) at 1184 K                        |
| #2/Zn-1<br>$7.74 \times 10^{-3}$                     | 50.3                               | 0.066                       | 0.029          | 0.008          | 50.03 (3) at 1122 K                         |
| #3/Zn-0<br>$1.87 \times 10^{-3}$                     | 50.0                               | 0.013                       | 0.006          | 0.002          | 49.50 (9) at 1064 K                         |
| #4/Zn-0<br>$32.79 \times 10^{-3}$                    | 50.0                               | 0.203                       | 0.084          | 0.035          | 49.69 (9) at 1225 K                         |

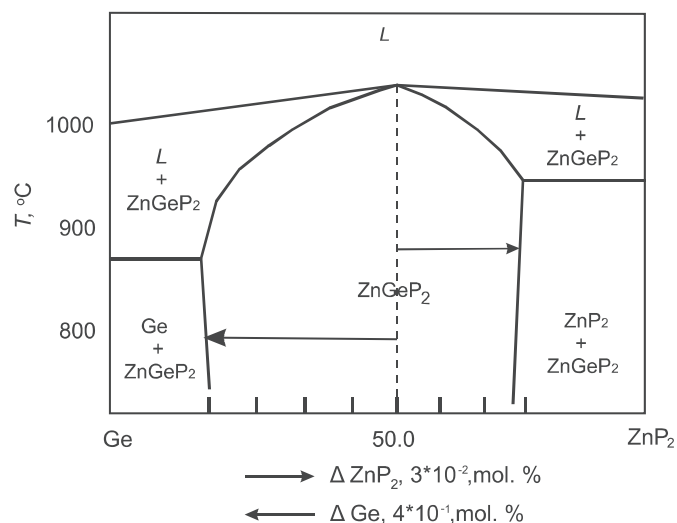


**Fig. 5.** The nonstoichiometry of ZnGeP<sub>2</sub> on the  $T$ - $x$  diagram of the ZnP<sub>2</sub>-Ge system.

the homogeneity range finding its equilibrium vapor pressure at a given temperature.

We will finally consider the tensimetric results in terms of defect chemistry. It was shown that along the section ZnP<sub>2</sub>-Ge the solid ZGP is in thermodynamic equilibrium with surrounding gaseous medium of ZnP<sub>2</sub> involving the Zn, P<sub>4</sub> and P<sub>2</sub> species with Zn/P=0.5. The deviation from stoichiometric composition is extended to both the ZnP<sub>2</sub> and Ge sides. Fig. 5 shows schematically the nonstoichiometry of ZGP on the  $T$ - $x$  diagram of the ZnP<sub>2</sub>-Ge system as the projection of the  $p$ - $T$ - $x$  diagram. Under high partial pressures the excess ZnP<sub>2</sub> (0.03%) is absorbed on the crystal surface and neutral vacancies are formed in the Ge sublattice running up to a maximal concentration of  $1.3 \times 10^{19} \text{ cm}^{-3}$ . Under low pressures any amount of ZnP<sub>2</sub> (maximal value is 0.40%) passes into the gaseous phase generating neutral Zn and P vacancies running up to  $5.6 \times 10^{21}$  and  $1.2 \times 10^{22} \text{ cm}^{-3}$ , respectively, due to the formula:  $X \text{ atom} \cdot \text{cm}^{-3} = X \text{ at} \% N/100$ , where  $N=n/V$  is the total number of atoms in 1 cm<sup>3</sup>.

According to the general theory of semiconductors disorder [17,18], charged vacancies ionized differently and associates formed by the Coulomb interaction between the positive and negative vacancies take also part in disorder of ZGP. The associates are formed due to high concentration of these vacancies, and their stability and dissociation into single vacancies are determined by the average distance between the vacancies. The charge of the associates may be neutral (annihila-

tion of the defects) or ionized if additionally the substitution (antisite) defects occur. It is clear that nature and concentration of all these defects are determined by temperature and the partial pressure of ZnP<sub>2</sub> in the form of different power functions.

Another approach describing the disorder of ZGP has been early based on the analysis of the annealing behavior and the measurements of photoluminescence, photoconductivity, optical absorption spectra, detected by magnetic resonance of the ZGP crystals. That the point defect chemistry of ZGP crystals is really quite complex has been shown by many previous investigations [6,9,19–21]. The Ge-deficient compositions are generated during high pressure physical vapor transport since the vapor of a molten source of ZGP is supersaturated near by the substrate [9]. The presence of phosphorus and zinc point defects and the acceptor and donor levels in the band gap is typical for the ZGP crystals grown from melt by horizontal gradient freezing and the Bridgman technique [6,9,19–21]. A significant reduction in the near-infrared absorption in the course of the annealing at 500 °C of ZGP crystals was connected with annihilation of defects [6]. Coulomb interaction between ionized donor-acceptor complexes and D-A transitions involving P<sub>Ge</sub> donor states and Ge□, Zn□ (□ is a vacancy), or Zn<sub>Ge</sub> acceptor states were considered in [6,9].

Our results based on defect models of the nonstoichiometric ZGP are in agreement with the results studying the defects by different physical methods. Earlier it has been shown that the zinc and phosphorus vacancies and the Ge antisite (Ge<sub>Zn</sub>) defects contribute mainly to the absorption of ZGP from fundamental absorption edge  $\sim 2.0$ – $\sim 0.5$  eV. Therefore, nonstoichiometry determined in the study as a function of partial pressures of Zn, P<sub>4</sub> and P<sub>2</sub> volatile species at different temperatures adding definite amounts of binary ZnP<sub>2</sub> opens a possibility to achieve uniform stoichiometry and, hence, in improving of the optical transparency in ZGP crystals.

#### 4. Summary

All the literature data up to date on the nonstoichiometry of ZnGeP<sub>2</sub> have been limited the to 1–10 mol% ZnP<sub>2</sub>. In the present study we have increased the detection limit of the solid solubility using a high sensitive static tensimetric method combined with precise determination of the phase purity and real composition of samples of the system ZnP<sub>2</sub>-Ge. The evaporation of the samples enriched by ZnP<sub>2</sub> or Ge were systematic and reproducible studied in the temperature range of 300–1200 K. The maximum solid solubility of ZnP<sub>2</sub> and Ge in ZnGeP<sub>2</sub> as 0.03% and 0.40% correspondingly was determined analyzing the  $P=P(x,T)_{r=2}$  (divariant equilibrium) and  $P=P(T)_{r=3}$  (monovariant equilibrium) dependences. The precise determination of stoichiometric ZnGeP<sub>2</sub>, nonstoichiometric ZnGeP<sub>2</sub>+ZnP<sub>2</sub> and ZnGeP<sub>2</sub>+Ge starting

compositions as well as compositions, calculated from the coordinates of the inflection points at the moment of changing of phase state of the system showed a good agreement supporting reliability of the results. Overall concentrations, dominant native defects and the vapor pressure necessary to keep stoichiometry of ZnGeP<sub>2</sub> crystals during the growth and annealing are evaluated.

## References

- [1] D.N. Nicogosjan, Materials for nonlinear optics, *Quantum Electron.* 4 (1971) 5.
- [2] J.L. Shay, J.H. Wernick, Ternary Chalcopyrite Semiconductors: Growth, Electronic Properties, and Applications, Pergamon Press, New York, 1975, p. 174.
- [3] A.S. Borshevskii, N.M. Shantsvoi, *Neorg. Mater. (Russia)* 1 (1975) 2158.
- [4] S. Fiechter, R. Castleberry, G. Wood, K. Bachman, in: R. Sciffman (Ed.), Proceedings of the 6th International Symposium on Experimental Methods for Microgravity Materials Science, 123, TMS Annual Meeting, San Francisco, 1994, p. 93.
- [5] S. Fiechter, R. Castleberry, N. Dietz, K. Bachman, H. Banks, K. Ito, J. Scroggs, H. Tran, in: Proceedings of 7th International Symposium on Experimental Methods for Microgravity Materials Science, 124 Annual Meeting of TMS, Las Vegas, 1994, p. 57.
- [6] S. Fiechter, R. Castleberry, M. Angelow, K. Bachman, in: M. Manasreh, T. Myers, F. Julien (Eds), Proceedings of the IR Applications of Semiconductors Materials, Processing and Devices, vol. 450, Pennsylvania, 1997, p. 315.
- [7] E. Buehler, J. Wernick, *J. Electron. Mater.* 2 (1973) 445.
- [8] L.I. Berger, V.D. Prochukhan, Ternary Diamond-like Semiconductors, Publishing House Moscow, Metallurgy, 1968, 151 pp.
- [9] N. Dietz, I. Tsveybak, W. Rudermann, G. Wood, K. Bachmann, *Appl. Phys. Lett.* 65 (1994) 2759.
- [10] V.B. Lazarev, J.H. Greenberg, B.A. Popovkin, *Current Topics in Materials Science*, 1978, p. 657 (Chapter 9).
- [11] G.A. Verozubova, A.I. Gribenyukov, Yu.P. Mironov, *Neorg. Mater.* 43 (2007) 1040.
- [12] G.A. Verozubova, A.I. Gribenyukov, in: *Crystallography Reports*, vol. 53, Pleades Publishing Inc., 2008, p. 158.
- [13] G.A. Ilinskii, Determination of Mineral Density, Publishing House Nedra, Leningrad, 1975, p. 119.
- [14] A. Alichanyan, A. Steblevski, Ja. Grinberg, S. Marenkin, G. Magomedzhaev, V. Gorgoraki, *Neorg. Mater.* 14 (1978) 1966.
- [15] V. Lasarev, Ya. Grinberg, S. Marenkin, G. Magomedzhaev, S. Samiev, *Neorg. Mater.* 14 (1978) 1961.
- [16] V. Titov, V. Kosyakov, F. Kuznetsov, Problems of the Electronic Materials, Science Nauka, Novosibirsk, 1986, p. 8.
- [17] H. Mott, G. Hery, Electronic processes in ionic crystals, Publishing House Inostranaja Literatura (1950).
- [18] F.A. Kröger, The Chemistry of Imperfect Crystals, North-Holland Publishing Company, Amsterdam, 1964, p. 187 (Chapter IX).
- [19] Kevin T. Zawilski, Peter G. Schunemann, Scott D. Setzler, Thomas M. Pollak, *J. Crystal Growth* 310 (2008) 1891.
- [20] Xin Zhao, Shifu Zhu, Beijun Zhao, Baojun Chen, Zhiyu He, R. Wang, Huiguang Yang, Yongqiang Sun, Jiang Cheng, *J. Crystal Growth* 311 (2008) 190.
- [21] D. Hofmann, N. Romanov, W. Gehlhoff, D. Pfisterer, B. Meyer, D. Azamat, A. Hofmann, *Physica B* 340–342 (2003) 978.